two-Tier 360-Degree Video Delivery Control in Multiuser Immersive Communications Systems

Ming Hu, Lifeng Wang, Bo Tan, and Shi Jin

***Abstract*—In the immersive communications systems, video information is stringently delivered for extended reality applications. Since users may demand various immersive experience and have different levels of view prediction accuracy, the two-tier video delivery frame structure with dynamic transmission time interval size needs to be designed appropriately. To maximize the system's quality of experience, new frame structures and power control are proposed. Meanwhile, the synchronous and asynchronous cases with different computational complexities are addressed. The results demonstrate the effectiveness of the proposed design and indicate that more flexible frame structure is beneficial for multiuser immersive communications.**

***Index Terms*—Immersive communications, quality of experience, frame structure, power control.**

I. Introduction

Immersive communications aim to achieve reality emulation and its beyond through interactions with remote participants and environments [1], which enable many extended reality (XR) applications such as video conferencing, immersive telepresence, remote assistance and maintenance etc. XR represents different types of realities including mixed reality (MR), virtual reality (VR), augmented reality (AR) and their interpolations, which has become one of the most important media applications in the industry, and 3GPP has attempted to evaluate the XR transmission methodologies in 5G networks [2]. Moreover, XR services are envisioned as the dominant use case in 6G [3].

In order to support ubiquitous immersive communications, the latency, computation cost and energy consumption are required to be much lower [4]. Since radio resources and computing capabilities are limited, it is imperative that the immersive system architectures shall be delicately designed. As a key component of immersive communications, video delivery mechanisms have attracted much attention. In [5], multicasting multi-view video contents are delivered to a collection of heterogeneous clients with diverse packet loss and the joint source and channel coding decisions are optimized to address the packet loss across the unreliable client access links. The multicasting multi-view video transmissions are also studied in [6], where the average weighted sum energy consumption is minimized by optimizing the view selection and transmission time and power allocation for given quality requirements of all users. Compared with the traditional single-tier solution under dynamic network conditions, [7] shows that a basic tier with the entire 360° video at a low rate allows users' field of views (FoVs) to be more smoothly rendered. In the case of multiple viewpoints, a multiple choice multiple dimensional knapsack problem is addressed in [8] such that the average tolerant delay for VR delivery is maximized. In [9], a deep-learning aided scheme is proposed to maximize the quality of delivering the VR wireless videos, where the multiuser scheduling subproblem is solved by using a matching theory approach. In [10], the energy consumption for AR applications is minimized by optimizing both communication and computation resources . To minimize the average required transmission rate, [11] formulates a joint caching and computing optimization problem of caching FoVs in 2D or 3D, in which the communications-caching-computing resources can be balanced. The use of millimeter wave (mmWave) bandwidths for delivering the panoramic VR video is considered in [12], where mobile edge computing (MEC) is an intermediate processing component to cut the energy consumption of the user equipment (UE). The recent work [13] focuses on the drone-assisted MEC network for high-quality mobile 360° video VR applications and maximize the users' quality of experience (QoE) via appropriate communications and computing resources.

Motivated by the above studies, we develop novel synchronous and asynchronous frame structures consisting of basic tier (BT) and enhancement tier (ET) for video delivery in multiuser mmWave cellular systems, where BT is adopted to improve the robustness against the FoV prediction failure. The prior work [7] considers a single user case and analyzes the optimal transmission rate values of BT and ET for QoE maximization in the absence of addressing the specific radio resource allocation. Unlike [7], we seek to maximize the overall QoE of the considered system and determine each UE's optimal transmission tim interval (TTI) durations and transmit power values of BT and ET video chunks in a frame.

II. System Description

A multiuser mmWave downlink system is considered, where the mmWave base station (BS) sends 360° video information requested by N UEs in a cell. To avoid the intra-cell interference resulted from the same beam conflict and keep user fairness, the channels between the BS and UEs are orthogonally divided in the frequency-domain with equal mmWave bandwidths. The binary parameter x_n $(n = 1, \cdots, N)$ indicates whether the n-th UE is associated with the BS ($x_n = 1$) or not ($x_n = 0$). Each frame is partitioned into BT video chunk phase and ET video chunk phase. As depicted in Fig. 1, we propose two different frame structures, namely synchronous and asynchronous cases. In the synchronous case, all the UEs have the same BT TTI size and ET TTI size; in the asynchronous case, the frame structure becomes more flexible since UEs may have different TTI sizes for BT/ET chunks.

M. Hu and L. Wang are with the Department of Electrical Engineering, Fudan University, Shanghai, China (E-mail: lifengwang@fudan.edu.cn).

B. Tan is with the Faculty of Information Technology and Communication Sciences, Tampere University, Finland (E-mail: bo.tan@tuni.fi).

S. Jin is with the Faculty of the National Mobile Communications Research Laboratory, Southeast University, Nanjing, China (E-mail: jinshi@seu.edu.cn).

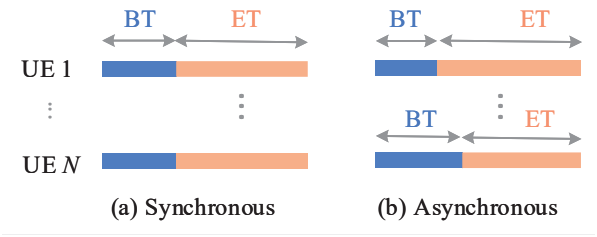

Fig. 1. The frame structures of two-tier video delivery systems: a) Same BT TTI size for all the UEs (synchronous); b) different BT TTI sizes for different UEs (asynchronous).

As a key performance metric in the immersive communications systems, QoE is widely represented as a logarithmic model. Therefore, given the normalized video rate $\hat{R}_n$ (bits/pixel), QoE of the n-th UE is given by [7, 14]

$$Q_n\left(\hat{R}_n\right) = a_n + b_n \log\left(\hat{R}_n\right), \tag{1}$$

where the constant parameters a_n and b_n depend on the specific XR video required by the n-th UE, $\hat{R}_n = \frac{R_n}{\mathcal{C}}$ with the transmission rate R_n (bits/s) and the coverage area of the video $\mathcal{C}$. Since the two-tier video delivery mechanism is adopted, BT chunk ensures that the UE's FoV can still be smoothly rendered when the FoV prediction is inaccurate. Based on (1), the QoE for the n-th UE in the considered two-tier video delivery system is calculated as

$$\widetilde{Q}_n = (1-q_n)\, Q_n\left(\hat{R}_n^{\mathrm{BT}}\right) + q_n Q_n\left(\underbrace{\hat{R}_n^{\mathrm{BT}} + \hat{R}_n^{\mathrm{ET}}}_{\Theta}\right), \tag{2}$$

where q_n $(0 \le q_n \le 1)$ is the hit probability that the FoV is accurately predicted, $\hat{R}_n^{\mathrm{BT}} = \frac{R_n^{\mathrm{BT}}}{\mathcal{C}^{\mathrm{BT}}}$ with the BT's transmission rate R_n^{BT} (bits/s) and the coverage area of the 360° video $\mathcal{C}^{\mathrm{BT}}$, and $\hat{R}_n^{\mathrm{ET}} = \frac{R_n^{\mathrm{ET}}}{\mathcal{C}^{\mathrm{ET}}}$ with the ET's transmission rate R_n^{ET} (bits/s) and the coverage area of the ET chunk $\mathcal{C}^{\mathrm{ET}}$, Θ denotes the effective rate after using layered coding to generate the ET chunks. The BT and ET's transmission rates R_n^{BT} and R_n^{ET} are

$$R_n^{\mathrm{BT}} = \rho_n^{\mathrm{BT}} B \log_2\left(1 + \frac{G_{\mathrm{t}} G_{\mathrm{r}} \left|\hbar_n^{\mathrm{BT}}\right|^2 p_n}{\delta^2}\right), \tag{3}$$

and

$$R_n^{\mathrm{ET}} = \rho_n^{\mathrm{ET}} B \log_2\left(1 + \frac{G_{\mathrm{t}} G_{\mathrm{r}} \left|\hbar_n^{\mathrm{ET}}\right|^2 p_n}{\delta^2}\right), \tag{4}$$

respectively, where ρ_n^{BT} $(0 < \rho_n^{\mathrm{BT}} \le 1)$ is the fraction factor to describe the BT's TTI in each frame, B is the bandwidth, $\rho_n^{\mathrm{ET}} = 1 - \rho_n^{\mathrm{BT}}$, G_{t} and G_{r} are the effective transmit antenna gain and receive antenna gain, respectively, $\left|\hbar_n^{\mathrm{BT}}\right|^2$ and $\left|\hbar_n^{\mathrm{ET}}\right|^2$ are the large-scale fading channel power gains[1], p_n is the transmit power spectral density (PSD) of the downlink channel between the BS and the n-th UE, and δ^2 is the noise's PSD. Without loss of generality, we assume that all the UEs obtain the same antenna gains.

[1]In the highly directional mmWave transmissions, the effect of small-scale fading is negligible.

Our goal is to maximize the system's QoE under the minimum QoE per UE constraint. To this end, we need to determine the optimal user association, BT and ET's TTI sizes and transmit PSD values. Therefore, the problem is formulated as

$$\begin{aligned}
\max_{\boldsymbol{x},\boldsymbol{\rho},\boldsymbol{p}} \ & \sum_{n=1}^{N} x_n \widetilde{Q}_n \qquad (5)\\
\text{s.t. } & \mathrm{C1}: x_n \in \{0,1\}, \quad \forall n,\\
& \mathrm{C2}: x_n\left(Q_n\left(\hat{R}_n^{\mathrm{BT}}\right) - \overline{Q}_n\right) \ge 0, \quad \forall n,\\
& \mathrm{C3}: \sum_{n=1}^{N} x_n p_n \le p_{\mathrm{total}},\\
& \mathrm{C4}: \rho_n^{\mathrm{BT}} + \rho_n^{\mathrm{ET}} = 1, \quad \forall n,\\
& \mathrm{C5}: \rho_n^{\mathrm{BT}} \ge 0, \rho_n^{\mathrm{ET}} \ge 0, p_n \ge 0, \quad \forall n,
\end{aligned}$$

where $\boldsymbol{x} = [x_n]$, $\boldsymbol{\rho} = [\rho_n^{\mathrm{BT}}, \rho_n^{\mathrm{ET}}]$, $\boldsymbol{p} = [p_n]$. Constraint C1 not only indicates the user association state but also guarantees that there always exist feasible solutions of the problem (5); constraint C2 makes sure that each associated UEs' QoE is satisfied, namely the BT video chunks can be successfully delivered to keep the minimum QoE level $\overline{Q}_n$; constraint C3 is the total transmit power constraint; constraint C4 describes the TTI sizes of the BT and ET.

III. Algorithm Design

The total QoE maximization problem (5) is a mixed-integer nonlinear programming (MINLP), which can be solved by using the computationally expensive enumeration methods. In this section, we design efficient solutions of problem (5) under synchronous and asynchronous circumstances. First, we adopt the linear programming (LP) relaxation, i.e., given $\{\boldsymbol{\rho}, \boldsymbol{p}\}$, the optimal user association is obtained by solving the LP subproblem as follows:

$$\begin{aligned}
\max_{\boldsymbol{x}} \ & \sum_{n=1}^{N} x_n \widetilde{Q}_n \qquad (6)\\
\text{s.t. } & \bar{\mathrm{C}}1: x_n \in [0,1], \quad \forall n,\\
& \mathrm{C2}, \quad \mathrm{C3}.
\end{aligned}$$

Then, we focus on the low-mobility scenario (namely $\left|\hbar_n^{\mathrm{BT}}\right|^2 = \left|\hbar_n^{\mathrm{ET}}\right|^2 = |\hbar_n|^2$), and seek to find the optimal BT and ET's TTI sizes and transmit PSD values for fixed $\boldsymbol{x}$.

A. Synchronous

Under the synchronous circumstance, all the UEs have the same BT and ET's TTI sizes, namely $\rho_n^{\mathrm{BT}} = \rho^{\mathrm{BT}}$ and $\rho_n^{\mathrm{ET}} = \rho^{\mathrm{ET}}$, $n = 1, \cdots, N$. By substituting (1)–(4) into (5), problem (5) with respect to (w.r.t.) $\{\boldsymbol{\rho}, \boldsymbol{p}\}$ can be equivalently transformed as

$$\max_{\boldsymbol{\rho},\boldsymbol{p}} \sum_{n=1}^{N} x_n \left((1-q_n)\, b_n \log \rho^{\mathrm{BT}} + q_n b_n \log\left(\frac{\rho^{\mathrm{BT}}}{\mathcal{C}^{\mathrm{BT}}} + \frac{\rho^{\mathrm{ET}}}{\mathcal{C}^{\mathrm{ET}}}\right) + b_n \log R_n\right) \tag{7}$$

$$\text{s.t. } \mathrm{C2}, \quad \mathrm{C3}, \quad \mathrm{C4}, \quad \mathrm{C5},$$

where $R_n = B \log_2\left(1 + \frac{G_{\mathrm{t}} G_{\mathrm{r}} |\hbar_n|^2 p_n}{\delta^2}\right)$. Although the subproblem (7) is convex, it is hard to get the closed-form

solution. Therefore, we attempt to solve it in a simple and effective manner. The Lagrange function of the subproblem (7) is given by

$$\begin{aligned}\mathcal{L}\left(\boldsymbol{\rho},\boldsymbol{p},\boldsymbol{\lambda},\mu,\nu\right)&=\sum_{n=1}^{N}x_n\left(1-q_n\right)b_n\log\rho^{\mathrm{BT}}\\&+\sum_{n=1}^{N}x_nq_nb_n\log\left(\frac{\rho^{\mathrm{BT}}}{\mathcal{C}^{\mathrm{BT}}}+\frac{\rho^{\mathrm{ET}}}{\mathcal{C}^{\mathrm{ET}}}\right)+\sum_{n=1}^{N}x_nb_n\log R_n\\&+\sum_{n=1}^{N}\lambda_nx_n\left(Q_n\left(\hat{R}_n^{\mathrm{BT}}\right)-\overline{Q}_n\right)\\&+\mu\left(p_{\mathrm{total}}-\sum_{n=1}^{N}x_np_n\right)+\nu\left(1-\rho^{\mathrm{BT}}-\rho^{\mathrm{ET}}\right),\end{aligned}\tag{8}$$

where $\boldsymbol{\lambda},\mu,\nu$ are non-negative Lagrange multipliers. Thus the KKT conditions for the subproblem (7) can be obtained as

$$\frac{\sum_{n=1}^{N}x_n\left(1-q_n+\lambda_n\right)b_n}{\rho^{\mathrm{BT}}}+\frac{\sum_{n=1}^{N}x_nq_nb_n}{\rho^{\mathrm{BT}}+\frac{\mathcal{C}^{\mathrm{BT}}}{\mathcal{C}^{\mathrm{ET}}}\rho^{\mathrm{ET}}}-\nu=0,\tag{9}$$

$$\frac{\sum_{n=1}^{N}x_nq_nb_n}{\rho^{\mathrm{BT}}\frac{\mathcal{C}^{\mathrm{ET}}}{\mathcal{C}^{\mathrm{BT}}}+\rho^{\mathrm{ET}}}-\nu=0,\tag{10}$$

$$x_n\left(b_n\Lambda\left(\lambda_n,\hbar_n,p_n\right)-\mu\right)=0,\tag{11}$$

$$\lambda_nx_n\left(Q_n\left(\hat{R}_n^{\mathrm{BT}}\right)-\overline{Q}_n\right)=0,\tag{12}$$

$$\mu\left(p_{\mathrm{total}}-\sum_{n=1}^{N}x_np_n\right)=0,\tag{13}$$

$$\nu\left(1-\rho^{\mathrm{BT}}-\rho^{\mathrm{ET}}\right)=0,\tag{14}$$

where $\Lambda\left(\lambda_n,\hbar_n,p_n\right)=\frac{(1+\lambda_n)}{R_n\log 2}\frac{BG_{\mathrm{t}}G_{\mathrm{r}}|\hbar_n|^2}{\delta^2+G_{\mathrm{t}}G_{\mathrm{r}}|\hbar_n|^2p_n}$ is a decreasing function of p_n. As such, we have the following remarks:

1) As $x_n=0$, it means that the n-th UE is inactive, therefore, $\rho^{\mathrm{BT}}=\rho^{\mathrm{ET}}=0$, $p_n=0$; As $x_n>0$, QoE constraint is also met as indicated from the subproblem (6), thus $\rho^{\mathrm{BT}}>0$ and $\nu>0$ according to (12) and (14). Under QoE constraint, the UE's minimum transmit PSD $p_{\min}$ satisfies $R_n|_{p_n=p_{\min}}=e^{\left(\overline{Q}_n-a_n\right)/b_n}$ with $\rho^{\mathrm{BT}}=1$.

2) Based on (9), (10) and (14), the optimal BT TTI satisfies

$$\rho^{\mathrm{BT}}=\min\left\{\left(1-\frac{\sum_{n=1}^{N}x_nq_nb_n}{\sum_{n=1}^{N}x_n\left(1+\lambda_n\right)b_n}\right)\frac{\mathcal{C}^{\mathrm{BT}}}{\mathcal{C}^{\mathrm{BT}}-\mathcal{C}^{\mathrm{ET}}},1\right\}.\tag{15}$$

Thus $\rho^{\mathrm{BT}}\in\left[\rho_{\min}^{\mathrm{BT}},1\right]$ with the minimum BT TTI $\rho_{\min}^{\mathrm{BT}}$ attained by letting $\lambda_n=0,\forall n$.

3) According to (9) and (10), an upper-bound of λ_n for fixed ρ^{BT} is given by

$$\lambda_n^{upper}=\sum_{n=1}^{N}\frac{x_nq_nb_n\rho^{\mathrm{BT}}b_{\min}^{-1}}{\rho^{\mathrm{BT}}\mathcal{C}^{\mathrm{ET}}+\mathcal{C}^{\mathrm{BT}}\rho^{\mathrm{ET}}}\left(\mathcal{C}^{\mathrm{BT}}-\mathcal{C}^{\mathrm{ET}}\right),\tag{16}$$

where $b_{\min}=\min_n b_n$.

4) It is seen from (11) that μ can be interpreted as the the water level for water-filling, which is a decreasing function of the transmit PSD p_n and an increasing function of λ_n. To make fast search, an upper-bound of μ is computed as $\mu_{\max}\le b_{\max}\Lambda_{\max}$, where $b_{\max}=\max_n b_n$ and $\Lambda_{\max}=\max_n\Lambda\left(\lambda_n^{upper},\hbar_n,p_{\min}\right)$.

5) Given ρ^{BT} and the water level μ, UE with $\lambda_n>0$ is given more transmit power than the case of $\lambda_n=0$ under the same channel condition according to (11). The reason is that as indicated in (12), $\lambda_n>0$ occurs when more transmit power has to be allocated to achieve the minimum QoE, namely $Q_n\left(\hat{R}_n^{\mathrm{BT}}\right)=\overline{Q}_n$, which is the worst-case for the associated UE due to the deep fading channel condition and lower quality level of the required video.

Lemma 1: Given a specific ρ^{BT} value, the feasible water level cannot be lower than μ_o, where μ_o is the root that satisfies (11) and (13) with $\rho^{\mathrm{BT}}=\rho_{\min}^{\mathrm{BT}}$.

Proof: Based on the **Remark 2**, $\rho^{\mathrm{BT}}=\rho_{\min}^{\mathrm{BT}}$ occurs when $\lambda_n=0,\forall n$, in this case, the water level $\mu=\mu_o$. Given a specific ρ^{BT} value, let Φ_i denote the set of UEs that satisfy QoE constraint with $\lambda_i=0$. If the feasible water level is lower than μ_o, the transmit PSD of the UEs in Φ_i increases according to (11) since $\lambda_i=0$, however, based on the **Remark 5**, the UEs with $\lambda_n\neq 0$ cannot keep $\lambda_n>0$, otherwise the total transmit power constraint (13) is violated. Thus **Lemma 1** is proved. ■

Based on the above remarks and **Lemma 1**, the proposed solution of the subproblem (7) is described in **Algorithm 1**.

Algorithm 1 Optimal algorithm for solving subproblem (7)

Step 1: Check the positive values $\{x_n\}$ (associated UEs) of the solution for subproblem (6). Let $\rho^{\mathrm{BT}}=\rho_{\min}^{\mathrm{BT}}$ (namely $\lambda_n=0,\forall n$), the water level μ_o is easily obtained via bisection search method according to (11) and (13), thus $\{p_n\}$ values are correspondingly computed according to (11), if $Q_n\left(\hat{R}_n^{\mathrm{BT}}\right)\ge\overline{Q}_n$, $\forall x_n>0$, the optimal solution is obtained. Otherwise, go to Step 2.

Step 2: Let $\mu_{\mathrm{L}}=\mu_o$ and $\mu_{\mathrm{H}}=\mu_{\max}$, Loop:
(1) Given the new water level $\mu=\mu_{\mathrm{m}}=\left(\mu_{\mathrm{L}}+\mu_{\mathrm{H}}\right)/2$, update ρ^{BT} and $\{p_n\}$ for satisfying (12)–(13) according to **Algorithm 2**, and substituting the updated ρ^{BT} and $\{p_n\}$ into (11) yields the updated $\{\lambda_n\}$.
(2) If the updated ρ^{BT} is equal to the (15) with the updated $\{\lambda_n\}$, the optimal solution that satisfies KKT conditions is obtained, and if the updated ρ^{BT} is larger than the (15) with the updated $\{\lambda_n\}$, update $\mu_{\mathrm{L}}=\mu_{\mathrm{m}}$. Otherwise, update $\mu_{\mathrm{H}}=\mu_{\mathrm{m}}$.

B. Asynchronous

Under the asynchronous circumstance, UEs are allowed to have different BT and ET's TTI sizes. Similar to III-A, the KKT conditions of problem (5) w.r.t. $\{\boldsymbol{\rho},\boldsymbol{p}\}$ are

$$x_n\left(1-q_n+\lambda_n\right)\frac{b_n}{\rho_n^{\mathrm{BT}}}+\frac{x_nq_nb_n}{\rho_n^{\mathrm{BT}}+\frac{C^{\mathrm{BT}}}{C^{\mathrm{ET}}}\rho_n^{\mathrm{ET}}}-\nu_n=0,\tag{17}$$

Algorithm 2 Bisection search w.r.t. ρ^{BT}

Step 1: Initialize $\rho_{\mathrm{L}}^{\mathrm{BT}}=\rho_{\min}^{\mathrm{BT}}$ and $\rho_{\mathrm{H}}^{\mathrm{BT}}=1$, Loop:

Step 2: Define $\rho_{\mathrm{m}}^{\mathrm{BT}}=\left(\rho_{\mathrm{L}}^{\mathrm{BT}}+\rho_{\mathrm{H}}^{\mathrm{BT}}\right)/2$. First, assume $\lambda_n=0$, $\forall n$, and compute UEs' $\{p_n\}$ based on (11) via Bisection search. Then, let Φ denote the set of associated UEs that satisfy $Q_i\left(\hat{R}_i^{\mathrm{BT}}\right)>\overline{Q}_i$ (namely QoE constraint is strictly achieved) with $\lambda_i=0$, and Φ' denote the set of the associated UEs with $Q_{i'}\left(\hat{R}_{i'}^{\mathrm{BT}}\right)\leq\overline{Q}_{i'}$ if $\lambda_{i'}=0$. Update $\{p_{i'}\}$ of the UEs in $\Phi_{i'}$ by computing $\left\{Q_{i'}\left(\hat{R}_{i'}^{\mathrm{BT}}\right)=\overline{Q}_{i'}\right\}$ to satisfy (12).

Step 3: If $\sum_{i\in\Phi}x_ip_i+\sum_{i'\in\Phi'}x_{i'}p_{i'}=p_{\mathrm{total}}$, the desired ρ^{BT} and corresponding $\{p_n\}$ for satisfying (12)–(13) values are got, and if $\sum_{i\in\Phi}x_ip_i+\sum_{i'\in\Phi'}x_{i'}p_{i'}<p_{\mathrm{total}}$, update $\rho_{\mathrm{H}}^{\mathrm{BT}}=\rho_{\mathrm{m}}^{\mathrm{BT}}$. Otherwise, update $\rho_{\mathrm{L}}^{\mathrm{BT}}=\rho_{\mathrm{m}}^{\mathrm{BT}}$.

$$\frac{x_nq_nb_n}{\rho_n^{\mathrm{BT}}\frac{\mathcal{C}^{\mathrm{ET}}}{\mathcal{C}^{\mathrm{BT}}}+\rho_n^{\mathrm{ET}}}-\nu_n=0, \tag{18}$$

$$\text{eq. (11), (12), (13),}$$

$$\nu_n\left(1-\rho_n^{\mathrm{BT}}-\rho_n^{\mathrm{ET}}\right)=0. \tag{19}$$

Like the **Remark 2**, each UE's optimal BT TTI satisfies

$$\rho_n^{\mathrm{BT}}=\min\left\{\left(1-\frac{q_n}{1+\lambda_n}\right)\frac{\mathcal{C}^{\mathrm{BT}}}{\mathcal{C}^{\mathrm{BT}}-\mathcal{C}^{\mathrm{ET}}},1\right\}. \tag{20}$$

Thus $\rho_n^{\mathrm{BT}}\in\left[\rho_{\min}^{\mathrm{BT}},1\right]$ with the minimum BT TTI $\rho_{\min}^{\mathrm{BT}}$ attained by letting $\lambda_n=0$, and ρ_n^{BT} is an increasing function of λ_n. Therefore, the proposed solution of the subproblem (7) is summarized in **Algorithm 3**.

Compared with the optimal solution in the synchronous circumstance, $N-1$ additional variables need to be optimized in the asynchronous circumstance. Therefore, the computation cost of the asynchronous frame design is higher, as seen in the **Algorithm 3** where it requires more Bisection search operations. [15]

After obtaining the optimal $\{\boldsymbol{\rho}^*,\boldsymbol{p}^*\}$ by using **Algorithm 1** for synchronous frame design or **Algorithm 3** for asynchronous frame design, substituting these optimal values into the subproblem (6) can update the $\boldsymbol{x}$ during each iteration, which is stopped until the objective function cannot be further improved. Thus the optimal $\boldsymbol{x}^*$ is obtained by rounding the ultimate solution of subproblem (6). Convergence of the proposed algorithms is guaranteed since the total QoE is an increasing function of the iteration index.

IV. Numerical Results

This section presents numerical results to confirm the efficiency of the proposed designs. In the simulations, the communication distance $d_n\geq 1$ from the BS to the n-th UE is uniformly distributed with the cell radius 200m, the hit probability q_n follows the normal distribution, and $a_n=0$, $b_n=1$, $\forall n$. The other basic simulation parameters are listed in Table I.

Algorithm 3 Optimal algorithm for solving subproblem (7)

Step 1: Check the positive values $\{x_n\}$ (associated UEs) of the solution for subproblem (6). Let $\rho_n^{\mathrm{BT}}=\rho_{\min}^{\mathrm{BT}}$ (namely $\lambda_n=0$), $\forall n$, the water level μ_o is easily obtained via bisection search method according to (11) and (13), thus $\{p_n\}$ values are correspondingly computed according to (11), if $Q_n\left(\hat{R}_n^{\mathrm{BT}}\right)\geq\overline{Q}_n$, $\forall x_n>0$, the optimal solution is obtained. Otherwise, go to Step 2.

Step 2: Let $\mu_{\mathrm{L}}=\mu_o$ and $\mu_{\mathrm{H}}=\mu_{\max}$, Loop:
(1) Let the new water level $\mu=\mu_{\mathrm{m}}=\left(\mu_{\mathrm{L}}+\mu_{\mathrm{H}}\right)/2$. First, assume $\lambda_n=0$, $\forall n$, and compute UEs' $\{p_n\}$ and ρ_n^{BT} based on (11) and (20), respectively. Then, let Φ denote the set of associated UEs that satisfy $Q_i\left(\hat{R}_i^{\mathrm{BT}}\right)>\overline{Q}_i$ with $\lambda_i=0$ and thus $\rho_i^{\mathrm{BT}}=\rho_{\min}^{\mathrm{BT}}$, and Φ' denote the set of the associated UEs with $Q_{i'}\left(\hat{R}_{i'}^{\mathrm{BT}}\right)\leq\overline{Q}_{i'}$ if $\lambda_{i'}=0$. Update $\{\lambda_{i'},\rho_{i'}^{\mathrm{BT}},p_{i'}\}$ of the UEs in $\Phi_{i'}$ by using bisection search w.r.t. $\lambda_{i'}$ to solve $\left\{Q_{i'}\left(\hat{R}_{i'}^{\mathrm{BT}}\right)=\overline{Q}_{i'}\right\}$ with (11) and (20), in order to satisfy (12).

Step 3: If $\sum_{i\in\Phi}x_ip_i+\sum_{i'\in\Phi'}x_{i'}p_{i'}=p_{\mathrm{total}}$, the desired solution for satisfying the KKT conditions is obtained, and if $\sum_{i\in\Phi}x_ip_i+\sum_{i'\in\Phi'}x_{i'}p_{i'}<p_{\mathrm{total}}$, update $\mu_{\mathrm{H}}=\mu_{\mathrm{m}}$. Otherwise, update $\mu_{\mathrm{L}}=\mu_{\mathrm{m}}$.

TABLE I
Simulation parameters

BT view coverage	$\mathcal{C}^{\mathrm{BT}}=360^\circ\times180^\circ$
ET view coverage	$\mathcal{C}^{\mathrm{ET}}=135^\circ\times135^\circ$
mmWave carrier frequency	$f_c=28$GHz
System bandwidth	$B=\frac{1}{N}$GHz with the number of UEs N
Effective transmit antenna gain	$G_{\mathrm{t}}=15$dBi
Effective receive antenna gain	$G_{\mathrm{r}}=10$dBi
Large-scale channel fading power gain	$\lvert h_n\rvert^2=\left(\frac{3\times10^8}{4\pi f_c}\right)^2\times d_n^{-2}$
Noise's PSD	$\delta^2=-169$dBm/Hz
Total transmit PSD	$p_{\mathrm{total}}=-47$dBm/Hz
Vectors of UEs' minimum QoE levels	$\overline{\mathbf{Q}}_{1\times4}=[1,2.5,2.1,1.9]$ for 4 UEs; $\overline{\mathbf{Q}}_{1\times6}=\left[\overline{\mathbf{Q}}_{1\times4},1.5,2.1\right]$ for 6 UEs; $\overline{\mathbf{Q}}_{1\times8}=\left[\overline{\mathbf{Q}}_{1\times6},2.5,2.6\right]$ for 8 UEs; $\overline{\mathbf{Q}}_{1\times10}=\left[\overline{\mathbf{Q}}_{1\times8},1.8,2.8\right]$ for 10 UEs; $\overline{\mathbf{Q}}_{1\times12}=\left[\overline{\mathbf{Q}}_{1\times10},2.7,1.7\right]$ for 12 UEs

Fig. 2 shows the total QoE for different numbers of UEs. The proposed solutions with the synchronous and asynchronous frame structures outperform the benchmark (equal transmit PSD and BT TTI $\rho_n^{\mathrm{BT}}=1$ for each UE). The use of asynchronous frame structure achieves better QoE than the synchronous counterpart, since larger multiuser diversity gains are obtained. As seen in Fig. 2, the performance gap between the synchronous and asynchronous frame structures becomes larger when adding more UEs.

Fig. 3 shows the total QoE for different values of the total transmit PSD, where there are twelve UEs in a cell. Our proposed solutions achieves much better performance than the benchmark. The best performance is obtained by the asynchronous frame design, thanks to larger multiuser diversity gains.

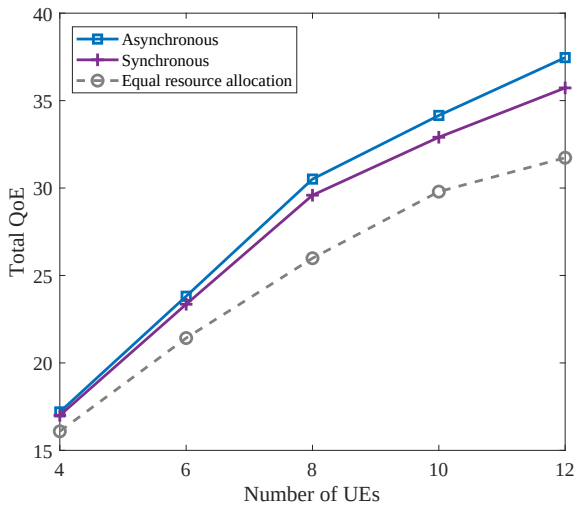

Fig. 2. Total QoE versus number of UEs.

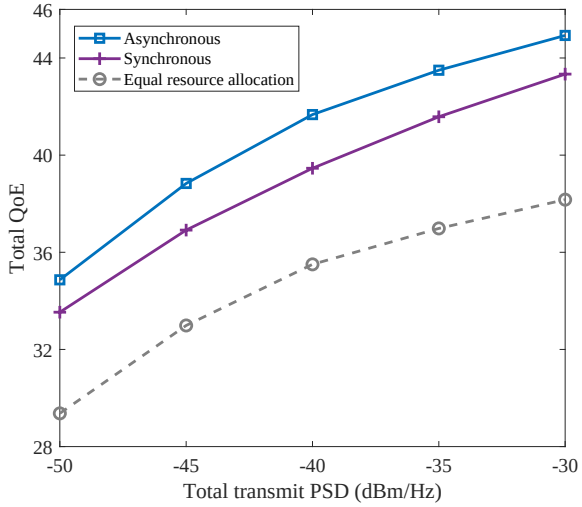

Fig. 3. Total QoE versus total transmit PSD.

V. Conclusion

In this paper, we proposed new frame structures for two-tier video delivery in multiuser immersive communications systems, to exploit the benefits of designing flexible frame structure. The considered problem was formulated to maximize the total QoE under the minimum QoE constraint. We provided low-complexity algorithms to solve the problem. The results confirm that the proposed solutions achieve larger total QoE and more multiuser diversity gains via asynchronous frame structure, which means that more flexible frame structure is beneficial.

References

[1] J. G. Apostolopoulos, P. A. Chou, B. Culbertson, T. Kalker, M. D. Trott, and S. Wee, "The road to immersive communication," *Proc. IEEE*, vol. 100, no. 4, pp. 974–990, April 2012.

[2] 3GPP TR 38.838, "Study on XR (Extended Reality) Evaluations for NR (Release 17)," Dec. 2021.

[3] F. Tariq, M. R. A. Khandaker, K.-K. Wong, M. A. Imran, M. Bennis and M. Debbah, "A speculative study on 6G," *IEEE Wireless Commun.*, vol. 27, no. 4, pp. 118–125, Aug. 2020.

[4] L. U. Khan, W. Saad, D. Niyato, Z. Han, and C. S. Hong, "Digital-twin-enabled 6G: Vision, architectural trends, and future directions," *IEEE Commun. Mag.*, vol. 60, no. 1, pp. 74–80, Jan. 2022.

[5] J. Chakareski, V. Velisavljevic, and V. Stankovic, "View-popularity-driven joint source and channel coding of view and rate scalable multi-view video," *IEEE J. Sel. Top Signal Process.*, vol. 9, no. 3, pp. 474–486, Apr. 2015.

[6] W. Xu, Y. Cui, and Z. Liu, "Optimal multi-view video transmission in multiuser wireless networks by exploiting natural and view synthesis-enabled multicast opportunities," *IEEE Trans. Commun.*, vol. 68, no. 3, pp. 1494–1507, Mar. 2020.

[7] L. Sun, F. Duanmu, Y. Liu, Y. Wang, Y. Ye, H. Shi, and D. Dai, "A two-tier system for on-demand streaming of 360 degree video over dynamic networks," *IEEE J. Emerg. Sel. Topics Circuits Syst.*, vol. 9, no. 1, pp. 43–57, July 2019.

[8] T. Dang and M. Peng, "Joint radio communication, caching, and computing design for mobile virtual reality delivery in fog radio access networks," *IEEE J. Sel. Areas Commun.*, vol. 37, no. 7, pp. 1594–1607, July 2019.

[9] C. Perfecto, M. S. Elbamby, J. D. Ser, and M. Bennis, "Taming the latency in multi-user VR 360°: A QoE-aware deep learning-aided multicast framework," *IEEE Trans. Commun.*, vol. 68, no. 4, pp. 2491–2508, Apr. 2020.

[10] A. Al-Shuwaili and O. Simeone, "Energy-efficient resource allocation for mobile edge computing-based augmented reality applications," *IEEE Wireless Commun. Lett.*, vol. 6, no. 3, pp. 398–401, June 2017.

[11] Y. Sun, Z. Chen, M. Tao, and H. Liu, "Communications, caching, and computing for mobile virtual reality: Modeling and tradeoff," *IEEE Trans. Commun.*, vol. 67, no. 11, pp. 7573–7586, Nov. 2019.

[12] Y. Liu, J. Liu, A. Argyriou, and S. Ci, "MEC-assisted panoramic VR video streaming over millimeter wave mobile networks," *IEEE Trans. Multimedia*, vol. 21, no. 5, pp. 1302–1316, May 2019.

[13] L. Zhang and J. Chakareski, "UAV-assisted edge computing and streaming for wireless virtual reality: Analysis, algorithm design, and performance guarantees," *IEEE Trans. Veh. Technol.*, vol. 71, no. 3, pp. 3267–3275, Mar. 2022.

[14] N. Kan, J. Zou, C. Li, W. Dai, and H. Xiong, "Rapt360: Reinforcement learning-based rate adaptation for 360-degree video streaming with adaptive prediction and tiling," *IEEE Trans. Circuits Syst. Video Technol.*, vol. 32, no. 3, pp. 1607–1623, Mar. 2022.

[15] C. You, K. Huang, H. Chae, and B.-H. Kim, "Energy-efficient resource allocation for mobile-edge computation offloading," *IEEE Trans. Wireless Commun.*, vol. 16, no. 3, pp. 1397–1411, Mar. 2017.